*Machine Learning and Artificial Intelligence*
*A.J. Tallón-Ballesteros and C. Chen (Eds.)*

*doi:10.3233/FAIA200809*

# Navigation Signal Design and Ranging Performance Evaluation of Cn Band Based on Satellite-to-Ground Link

Xiaofei CHEN[a,b] , Xue WANG [a,b,1] , Xiaochun LU[a,b] , Jing KE [a,b] and Xia GUO [b]
[a] *University of Chinese Academy of Sciences*
[b] *National Time Service Center, Chinese Academy of Sciences*

**Abstract.** As the only priority frequency band for navigation services except L protected by ITU, the Cn band could provide navigation services to solve problems of spectrum congestion and vulnerability to interference faced in L using global navigation satellite systems. However, Cn band navigation still faces some problems such as limited-bandwidth and link uncertainty. To solve these problems, an orthogonal MSK signal is designed in this paper under Cn limited bandwidth constraint. The analysis results show that although it's ranging performance of narrow correlation spacing has been deteriorated, the performance of wide correlation spacing has been improved, and it can reduce 98.7% power interference to adjacent radio astronomy band. On the other hand, the Cn band navigation signal test based on the satellite-to-ground link is carried out in this paper. The test results show that the trend of designed signals' ranging performance is consistent with the simulation results and its rain attenuation is 0.5-1dB.

**Keywords.** Cn band, navigation, ranging performance, orthogonal MSK

## 1. Introduction

Global navigation satellite systems (GNSS), including GPS, GLONASS, Galileo, BDS and other region navigation systems, is the infrastructure in modern society, which provides navigation, positioning and timing services. Although it plays an essential role in many fields, it still has some drawbacks that are difficult to be solved. One of which is vulnerable to interference, and another is spectrum congestion. Due to the low receiving signal power, GNSS is easily interfered with strong signals. Moreover, it is not easy to provide more diversified services because of the L band frequency resources' limitation. As the only priority frequency band for navigation services other than L protected by ITU, the Cn band (5010MHz-5030MHz) could provide navigation services to alleviate the above problems effectively.

In 2000, Cn band navigation was initially proposed and intended to be used by the Galileo system [1, 2], and its benefits and drawbacks were studied [3]. However, due to the limitation of the satellite's power and equipment complexity and cost of Cn band compared with L, the Cn band navigation was given up, and the development of the Cn

[1] Corresponding Author: Researcher on Navigation. National Time Service Center, Shuyuan East Road 3, 710600 Lintong distinct Xian Shaanxi, China; E-mail: wangxue@ntsc.ac.cn.

band navigation were also restricted [4, 5]. With the development of technology, these problems are no longer restrictions, and as a critical resource, Cn band navigation has been paid attention again. Hein, G.W. etc. analyzed the feasibility of developing navigation services on the Cn band [6]. Guoxiang Ai etc. studied the feasibility of Cn band to provide high-precision services [7]. Thomas Jost etc. compared the navigation performance of L band and Cn band with ground test [8]. Yinjiang Yan etc. provided the rain attenuation analysis of C-band navigation signal [9]. Rui Xue etc. proposed continuous phase modulation to reduce signal sidelobes and analyzed its performance [10, 11]. Ying Wang etc. studied the technology and prospect of Cn band navigation [12]. Yanbo Sun etc. discussed the scheme for L/C dual-frequency combined navigation signal [13]. The compatibility of the Cn band with its adjacent service has also been studied [14]. However, this paper presents the current lack of the ranging performance evaluation results of the Cn band navigation based on the satellite-to-ground link.

This paper designed orthogonal MSK signal under Cn limited bandwidth constraint and provided the test results of designed signal based on satellite-to-ground link, revealing the ranging and link performance of Cn band used for navigation.

## 2. Signal Design

### *2.1. Carrier Frequency Selection*

Cn band and its adjacent telecommunication services are shown in fig.1. It can be seen that the Cn bandwidth is only 20MHz, its upper frequency sideband is the microwave landing service (MLS), and its lower frequency sideband is the radio astronomy service (RAS) and Galileo's uplink service. Generally, RAS is easily interfered and has stringent restrictions on in-band interference. Therefore, considering maximum utilization efficiency and reducing the interference to RAS, the carrier frequency should be selected at the center or the upper sideband close to it.

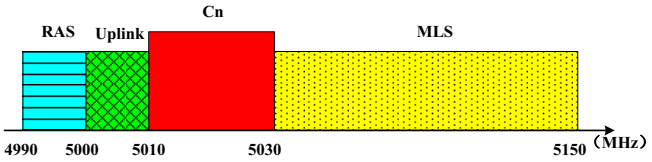


**Figure 1.** The frequency allocation of the Cn band and its adjacent service.

On the other hand, considering forward compatibility with GNSS and carrier and ranging code with the same frequency source to improve positioning accuracy, the carrier frequency must be an integer multiple of the ranging code frequency, and they all must be an integer multiple of 1.023MHz. Several alternative carrier frequencies are listed in table 1.

**Table 1.** Several alternative carrier frequencies.

| Code Frequency (MHz) | Multiple relationship with Code | Multiple relationship with 1.023M | Carrier Frequency (MHz) |
|---|---|---|---|
| 10.23 | 490 | 4900 | 5012.70 |
| 10.23 | 491 | 4910 | *5022.93* |
| 10.23 | 492 | 4920 | 5033.16 |

| Code Frequency (MHz) | Multiple relationship with Code | Multiple relationship with 1.023M | Carrier Frequency (MHz) |
|---|---|---|---|
| 5.115 | 980 | 4900 | 5012.70 |
| 5.115 | 981 | 4905 | 5017.815 |
| 5.115 | 982 | 4910 | *5022.93* |
| 2.046 | 2453 | 4906 | 5018.838 |
| 2.046 | 2454 | 4908 | 5020.884 |
| 2.046 | 2455 | 4910 | *5022.93* |

It can be seen in table 1 that the closest to the center frequency point is 5020.884MHz. However, the frequency could be gotten only one case, which brings many constraints to the signal design. While 5022.93MHz not only satisfies the many cases and increases flexibility in signal design, it also upper 2.93MHz than center frequency point, which could reduce the interference to RAS. According to these factors, the carrier frequency is selected as 5022.93MHz during the test.

Except this, the Cn band's rain attenuation also should be considered. According to reference [15], it would be reached from 0.26-4.61dB. Therefore, the influence of rain attenuation on the carrier-to-noise ratio also needs to be considered.

### *2.2. Band-limited Signal Design*

Generally, the satellite navigation system uses binary phase-shift keying (BPSK) modulation. It modulates two different pseudo-random noise (PRN) codes on the in-phase and quadrature respectively, which could be expressed as

$$s_{BPSK} = c_I g_I(t)\cos(2\pi f_c t) - c_Q g_Q(t)\sin(2\pi f_c t) \tag{1}$$

where $c_I$ and $c_Q$ are PRN codes, and their frequency are n*1.023MHz denoted as BPSK(n), which decide the bandwidth of the signal; $g_I(t)$ and $g_Q(t)$ are signal waveforms, and they are rectangular waveform, which decide the shape of the signal power spectrum; and $f_c$ is the carrier frequency, here is 5022.93MHz. Its power spectrum and baseband waveform are shown in Fig.2. Its signal constellation and phase change as following in Fig.3.

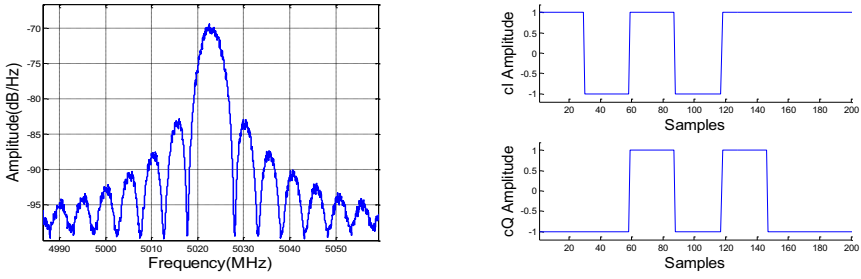


**Figure 2.** (a) BPSK (5) signal power spectrum; (b) BPSK (5) signal baseband waveform.

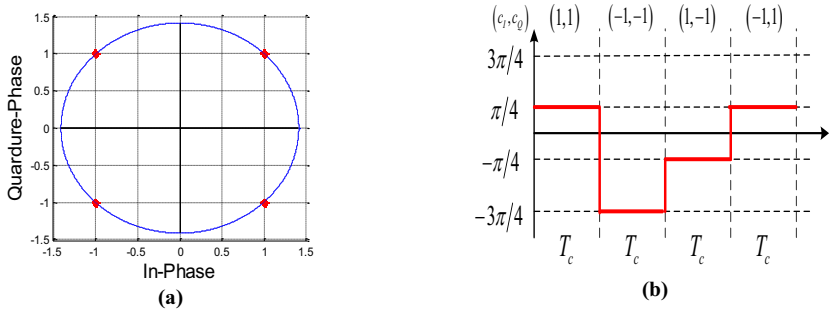


**Figure 3.** (a) BPSK (5) signal constellation; (b) BPSK (5) signal phase change.

Because of Cn band limited-bandwidth and compatibility, and to reduce the interference to adjacent services, especially RAS, it is necessary to reduce the power spectrum's sidelobes. From Fig.3 (b), it can be seen that phase jumping causes larger sidelobes. To reduce the sidelobes of the power spectrum, a kind of orthogonal MSK modulation is proposed based on the traditional MSK modulation. It delays $c_Q$ half chip compared with the $c_I$ and is denoted as

$$c_d = c_Q\left(t - T_c/2\right) \tag{2}$$

where $T_c$ is the duration time of one chip. Then the orthogonal MSK modulation could be expressed as

$$s_{O-MSK} = c_I \sin\left(\frac{\pi t}{T_c}\right)\cos\left(2\pi f_c t\right) - c_d \sin\left(\frac{\pi\left(t - T_c/2\right)}{T_c}\right)\sin\left(2\pi f_c t\right) \tag{3}$$

Its power spectrum and baseband waveform are shown in Fig 4. Fig.4 (a) describes that compared with BPSK, orthogonal MSK's power spectrum sidelobe has a significant drop. The power in the band of RAS is denoted as

$$P_{RAS} = \int_{4990\,MHz}^{5000\,MHz} G\left(f\right)df \tag{4}$$

where $G\left(f\right)$ is the power spectrum. Through calculation, the power in band of RAS for BPSK(5) is -45.69dBW, and for orthogonal MSK(5) is -64.5dBW, it is found that compared with BPSK, the power of orthogonal MSK in the RAS band is reduced by 98.7%. The baseband waveform of orthogonal MSK is shown in Fig.4 (b). It can be seen that the orthogonal MSK replaces the rectangular chip with a sinusoidal chip. The orthogonal MSK's phase could be expressed as

$$\theta(t)=\begin{cases}\left(-\dfrac{\pi t}{T_c}c_I+\dfrac{\pi}{2}\right)c_d, 0\le t<\dfrac{T_c}{2}\\ \left(\dfrac{\pi t}{T_c}c_I-\dfrac{\pi}{2}\right)c_d, \dfrac{T_c}{2}\le t<T_c\end{cases} \tag{5}$$

Its signal constellation and phase change as Fig.5 shown. It can be seen that its phase changes linearly with time and there is no phase jump.

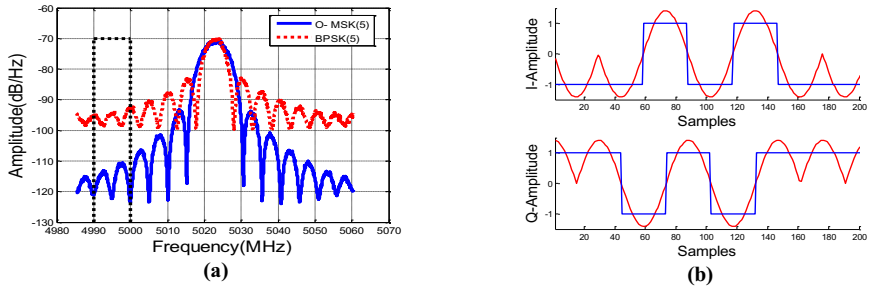


**Figure 4.** (a) Orthogonal MSK (5) signal power spectrum; (b) Orthogonal MSK (5) signal baseband waveform.

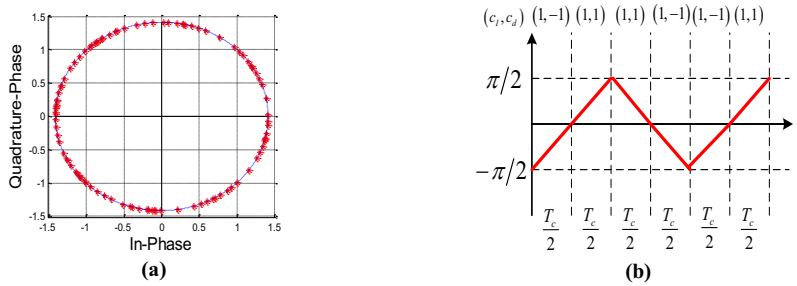


**Figure 5.** (a) Orthogonal MSK (5) signal constellation; (b) Orthogonal MSK (5) signal phase change.

The autocorrelation function curve determines the signal's receiving performance. Fig.6 reveals the autocorrelation function of the two signals. It can be seen that compared with BPSK, the correlation function of orthogonal MSK becomes smoother especially near the correlation peak.

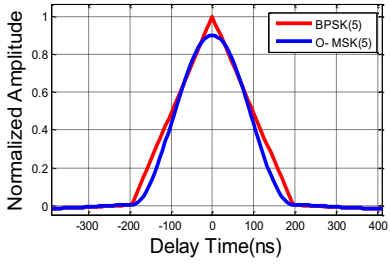


**Figure 6.** The autocorrelation function of BPSK (5) and orthogonal MSK (5).

### 2.3. Ranging Accuracy Analysis

With the ranging accuracy equation, signal's ranging theoretical performance can be easily to get [16].

$$\sigma^2 = \frac{B\left(1-0.25BT\right)\int_{-\beta/2}^{\beta/2} G_{s0}\left(f\right)\sin^2\left(\pi f\Delta\right)df}{\left(2\pi\right)^2\left(C/N_0\right)\left(\int_{-\beta/2}^{\beta/2} fG_{s0}\left(f\right)\sin\left(\pi f\Delta\right)df\right)^2} \times\left(1+\frac{\int_{-\beta/2}^{\beta/2} G_{s0}\left(f\right)\cos^2\left(\pi f\Delta\right)df}{T\left(C/N_0\right)\left(\int_{-\beta/2}^{\beta/2} G_{s0}\left(f\right)\cos\left(\pi f\Delta\right)df\right)^2}\right) \tag{6}$$

where $\beta$ is the radio frequency bandwidth and $B$ is the bandwidth of the code tracking loop; $G_{s0}\left(f\right)$ is the normalized power spectrum; $\Delta$ is the early-to-late spacing; $C/N_0$ is the carrier-to-noise ratio; $T$ is the correlation integration time. With the parameter of $\beta = 20MHz$, $B = 5Hz$, $\Delta = 200ns$, $T = 1ms$ and $C/N_0$ from $35dBHz$ to $50dBHz$, the ranging accuracy curve can be drawn as shown in Fig.7 (a). Changing its early-to-late spacing from 200ns to 20ns, the ranging accuracy curve can be drawn as shown in Fig.7 (b).

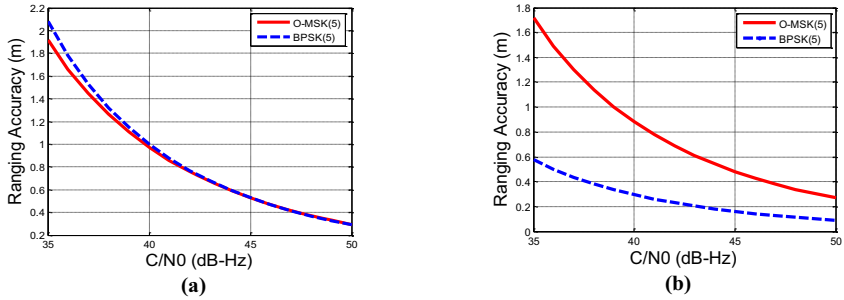


**Figure 7.** (a) The ranging accuracy of BPSK(5) and orthogonal MSK(5) with $C/N_0$ from 35 to50 dB-Hz and early-to-late spacing 200ns; (b) The ranging accuracy of BPSK(5) and orthogonal MSK(5) with $C/N_0$ from 35 to50 dB-Hz and early-to-late spacing 20ns.

Because of bandwidth limitation, orthogonal MSK (5) has more power in the bandwidth, and it could bring higher ranging accuracy in width correlation spacing -the early-to-late spacing more than 160ns- as Fig.7 (a) shown. While in narrow correlation spacing-the early-to-late spacing less than 160ns, the ranging accuracy of orthogonal MSK(5) becomes worse than BPSK(5), and that is because its autocorrelation curve becomes smoother and its anti-noise ability will be reduced as Fig.7(b) and Fig.6 shown. The ranging performance loss of narrow correlation spacing is the price to reduce the interference with out-of-band service.

## 3. Test Equipment and Methods

The testing system is shown in Fig.8, which includes signal generating equipment, transmitting antenna, on-orbit satellite, receiving antenna and equipment, and analysis equipment.

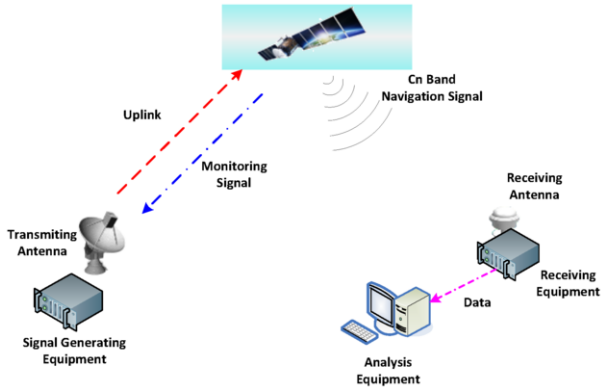


**Figure 8.** The testing equipment and interface between them.

The signal generating equipment generates the signal designed, including BPSK (5) and orthogonal MSK (5). The antenna transmits the generated signal by uplink and receives the monitoring signal to evaluate signal status. The satellite retransmits the Cn band navigation signal, and the receiving equipment receives it with an omnidirectional receiving antenna. Then the analysis equipment collects the pseudorange to analysis the signal's ranging performance. The signal generating equipment and receiving equipment are shown as Fig.9.

**(a)** **(b)**

**Figure 9.** Testing equipment: (a) signal generating equipment; (b) receiving equipment.

During the test, the BPSK (5) signal is transmitted by the signal generating equipment. At the same time, the monitored signal is correct and stable, receiving equipment records the carrier-to-noise ratio and pseudorange. Then altering the signal to orthogonal MSK (5) and repeat the above work. The monitoring spectrum of BPSK (5) and orthogonal MSK (5) are shown in Fig.10. It can be seen that compared with BPSK (5), orthogonal MSK (5)'s sidelobe have significantly reduced.

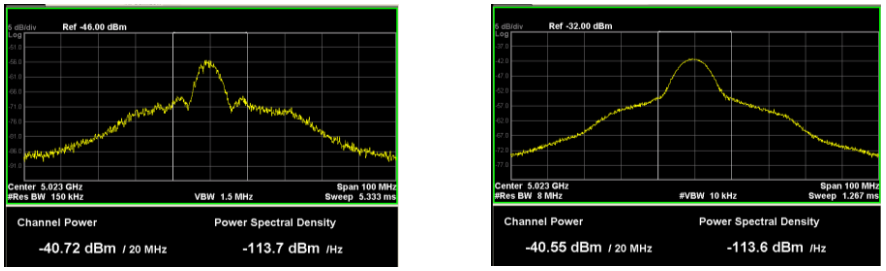


**(a)** **(b)**

**Figure 10.** (a) BPSK(5) monitoring signal; (b) Orthogonal MSK(5) monitoring signal.

## 4. Results Analysis

Two scenarios were designed to test the ranging performance and rain attenuation during the test respectively.

### *4.1. Ranging Performance*

Because the noise is a random variable, which is the main factor affecting the ranging performance and the satellite's motion following the Kepler equations, other variables are determined and changed slowly, the method based on high-order polynomial fitting can be used to measure the ranging performance. The receiving pseudorange $y_d$ is

$$y_d = \rho + \Delta\rho + n \tag{7}$$

where $\rho$ is the real range, and $\Delta\rho$ is the range bias, n is the thermal noise. Because $\rho + \Delta\rho$ could be fitted with an n-order polynomial,

$$y = a_0 + a_1 x + a_2 x^2 + \cdots + a_n x^n \tag{8}$$

then choose the polynomial to minimize the Eq. (9).

$$\min\{\mathrm{E}[y_d - y]\} = \min\left\{\mathrm{E}[\rho + \Delta\rho - y + n]\right\} \tag{9}$$

where $\mathrm{E}$ expresses the mean operation. As the polynomial fitting eliminates the bias, what is left is the variation that affects the ranging performance, and then the Eq. (10) could be used to reflect the ranging performance.

$$\sigma = \sqrt{\frac{\sum_{i=1}^{n}\left(y_d[i] - y\right)^2}{n-1}} \tag{10}$$

where $y_d[i]$ is the i[th] receiving pseudorange.

The parameter of the receiver was chosen as $\beta = 20MHz$, $B = 5Hz$, $\Delta = 200ns$, $T = 1ms$, and data time is 10 minutes, the test result of ranging performance as shown in Fig.11 and Fig.12.

The carrier-to-noise ratio (upper) and the ranging performance (lower) of orthogonal MSK(5) and BPSK(5) are shown in Fig.11 (a) and Fig.11 (b) respectively. It can be seen that the carrier-to-noise ratio changes around 45.5dB-Hz, the ranging performance of orthogonal MSK(5) is 0.7607m, BPSK(5) is 0.7919m. Fig.12 shows the test results with carrier-to-noise ratio changes around 42.5dB-Hz, and their ranging performance reduces to 1.0518m and 1.0595m respectively.

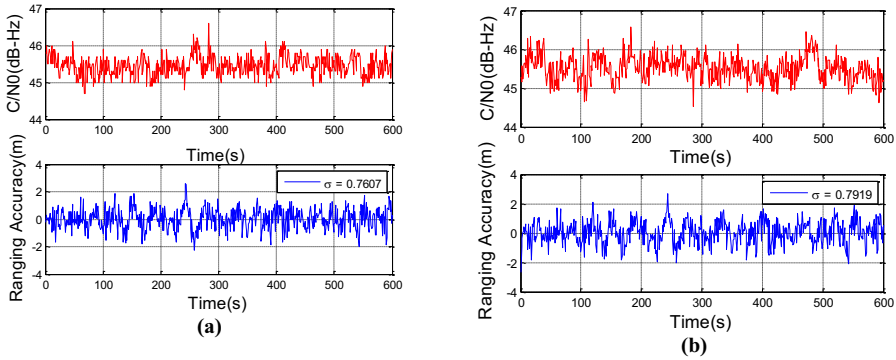


**Figure 11.** (a) The ranging performance of orthogonal MSK(5); (b) The ranging performance of BPSK(5).

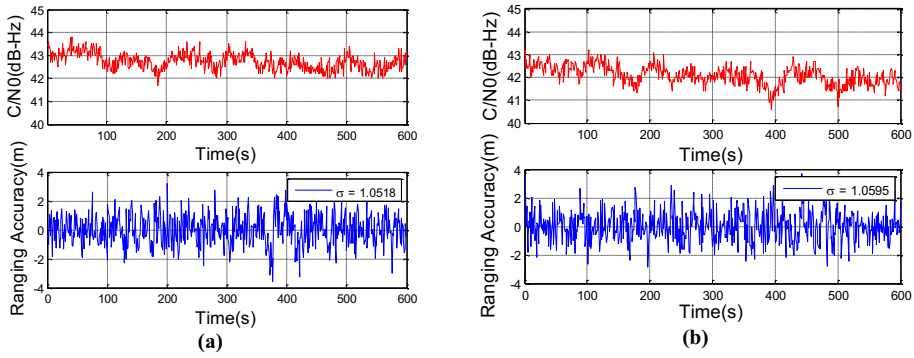


**Figure 12.** (a) The ranging performance of orthogonal MSK (5); (b) The ranging performance of BPSK (5).

Table 2 lists the ranging performance of simulation and test results with different carrier-to-noise to compare with test results and simulation results. It can be seen that the overall trend of test results is consistent with the simulation.

**Table 2.** The ranging performance of the two signals with different carrier-to-ratio.

| Carrier-to-noise Ratio | Orthogonal MSK (5) | | BPSK(5) | |
|---|---|---|---|---|
| | Simulation | Test Results | Simulation | Test Results |
| 45.5 dB-Hz | 0.4973m | 0.7607m | 0.4978m | 0.7919m |
| 42.5 dB-Hz | 0.7136m | 1.0518m | 0.7222m | 1.0595m |

### 4.2. Rain Attenuation

In order to test the rain attenuation of the Cn band, choose the same testing time and location on different days when it rains and not. The test environment is shown in Fig.13.

(a) (b)

**Figure 13.** (a) The omnidirectional receiving antenna when it rains; (b) The omnidirectional receiving antenna when it not.

Fig.14 shows the rain attenuation of the Cn band. There is the carrier-to-ratio of the receiver at the same testing time and location with orthogonal MSK (5) modulation on different days, the weather of the upper one is rain and the lower not. It can be seen that the rain attenuation is 0.5-1dB, which should be considered at the Cn band navigation system design.

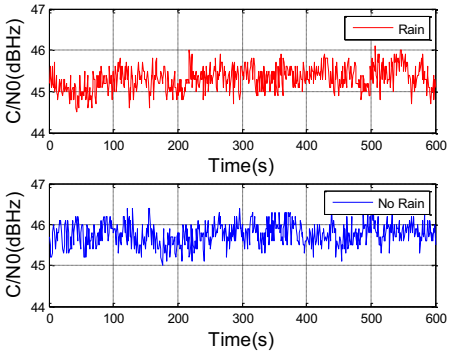


**Figure 14.** The test result of rain attenuation on the Cn band.

## 5. Conclusion

In this paper, a Cn band navigation signal test is carried out based on the satellite-to-ground link. It tested the ranging performance and link performance of the designed Cn band signals. The test results show that the ranging performance trend of the signals is consistent with the simulation, and its rain attenuation is 0.5-1dB. As an important frequency resource, the Cn band can be used for navigation service, but its rain attenuation should be considered at the Cn band navigation system design.

## References

[1] S.Loddo. Galileo Overall Architecture Definition Executive Summary, Issue 06, Dec 08, 2000.
[2] Lindenthal, W.etal. GalileoSat. C-Band Navigation Payload Space Segment Assessments, WP 3300, Astrium, 2001.
[3] Irsigler, M., Hein, G.W.&Schmitz-Peiffer,A. "Use of C-Band Frequencies for Satellite Navigation: Benefits and Drawbacks". GPS Solutions (2004): 119-139.
[4] J.A. Avila-Rodriguez, S.Wallner, J.H.Won,B.Eissfeller,A.Schmitz-Peiffer, J.J.Fl-och,E.Colzi,J.-L.Gerner. Study on a Galileo Signal and Service Plan for C-band, Proceedings of ION GNSS 2008, Savannah, Georgia, USA, 2008.
[5] Schmitz-Peiffer, A.,D.Felbach, F.Soualle, R.King, S.Paus, A.Fernandez, R.Jorgens-en, B.Eissfeller, J.A.Avila-Rodriguez, S.Wallner, T.Pany, J.H.Won, M.Anghileri, B.Lankl, E.Colzi. Assessment on the Use of C-Band for GNSS within the European GNSS Evolution Programme, Proceeding of ION GNSS 2008, Savannah, Georgia, USA, 2008.
[6] Hein, G.W., J.A.Avila-Rodriguez, S.Wallner, J.H.Won. "Architecture for a Future C-band/L-band GNSS Mission-Part2: Signal Considerations and Related User Terminal Aspects". Inside GNSS (2009):47-56.
[7] Guoxiang Ai, Lihua Ma, Huli Shi, Guanyi Ma, Ji Guo, Zhigang Li, Xiaohui Li, Haitao Wu, and Yujing Bian. "Achieving Centimeter Ranging Accuracy with Triple-frequency Signals in C-band Satellite Navigation Systems". Navigation 58, no. 1 (2011):59-68.
[8] Thomas Jost, Wei Wang, Uwe-Carsten Fiebig, and Fernando Perez-Fontan. "Comparison of L-and C-band Satellite-to-indoor Broadband Wave Propagation for Navigation Applications". IEEE transactions on antennas and propagation 59, no. 10 (2011): 3899-3909.
[9] Yinjiang Yan, Shuyu Zhang. "Rain Attenuation Analysis of C-Band Satellite Navigation Signal". Modern Navigation (2012): 157-159.
[10] Rui Xue, Qingming Cao, Qiang Wei. "A Flexible Modulation Scheme Design for C-Band GNSS Signals[J], Mathematical Problems in Engineering". 2015.pt.11.(2015): 165097.1-165097.8.
[11] Rui Xue, Huan Yu, and Qinglin Cheng. "Adaptive Coded Modulation Based on Continuous Phase Modulation for Inter-satellite Links of Global Navigation Satellite Systems". IEEE Access 6 (2018): 20652-20662.
[12] Ying Wang, Yansong Meng, Xiaoxia Tao, Lei Wang, Zhe Su. Study on Cn Band Satellite Navigation, China Satellite Navigation Conference 2016, Chang Sha, China, 2016.
[13] Yanbo Sun, Rui Xue, Dun Wang, et al. "General Modulation Scheme for L/C Dual-frequency Combined Navigation Signal". Journal of Harbin Engineering University (2018).
[14] Zhiyun Li, Yan Bai, Xiaochun Lu. "Rearch on Radio Frequency Compability Evaluation Method of Cn Band Navigation Signal". Journal of Time and Frequency (2019): Vol. 42, 0087-0096.
[15] Markus Irsigler, Günter W. Hein, Bernd Eissfeller,Andreas Schmitz-Peiffer etc. Aspects of C-band Satellite Navigation: Signal Propagation and Satellite Signal Tracking, Proceedings of the European Navigation, Conference ENC-GNSS 2002, Copenhagen, Denmark, 27-30 May 2002.
[16] Betz, J.W. Design and Performance of Code Tracking for the GPS M Code Signal. Proceedings of the 13th International Technical Meeting of the Satellite Division of the Institute of Navigation ION GNSS 2000, Salt Lack City, UT, 19-22 September 2000, 2140-2150.